

G.L. ZHAO\*, Y. ZOU\*<sup>‡</sup>, Y.L. HAO\*, Z.D. ZOU\*

## CORROSION RESISTANCE OF ELECTROLESS Ni-P/Cu/Ni-P MULTILAYER COATINGS

### ODPORNOŚĆ KOROZYJNA WIELOWARSTWOWYCH POWŁOK Ni-P/Cu/Ni-P NAKŁADANYCH METODĄ POWLEKANIA BEZPRĄDOWEGO

Ni-P/Cu/Ni-P multilayer coatings were prepared by deposition of Cu layer between two Ni-P layers. The Cu layer was deposited by metal displacement reaction between  $\text{Cu}^{2+}$  and Fe atoms. Corrosion behavior of single-layer Ni-P coatings, double-layer Ni-P/Cu coatings, and three-layer Ni-P/Cu/Ni-P coatings were investigated by electrochemical tests in 3.5% NaCl solution. The three-layer coatings exhibited more positive  $E_{corr}$  and decreased  $I_{corr}$  compared with conventional single-layer Ni-P coatings, which indicated an improved corrosion resistance. The polarization curves of the three-layer coatings were characterized by two passive regions. The improved corrosion resistance was not only attributed to the function of the blocked pores of Cu. The Cu interlayer also acted as a sacrificial layer instead of a barrier in the coatings, which altered the corrosion mechanism and further improved the corrosion resistance of the coatings.

*Keywords:* electroless plating, multilayer coatings, porosity, electrochemical tests, crystalline Cu layer

Wielowarstwowe powłoki Ni-P/Cu/Ni-P wytworzono metodą osadzania miedzi pomiędzy dwoma warstwami Ni-P. Warstwę Cu otrzymano dzięki reakcji wypierania metalu przez metal (dla miedzi i żelaza). Aby określić właściwości korozyjne jednowarstwowej powłoki Ni-P, dwuwarstwowej Ni-P/Cu oraz trójwarstwowej Ni-P/Cu/Ni-P przeprowadzono pomiary elektrochemiczne w 3,5% roztworze NaCl. Powłoki trójwarstwowe w porównaniu do jednowarstwowych wykazały się większą wartością  $E_{corr}$ , przy malejącej wartości  $I_{corr}$ . Wskazuje to na poprawę odporności na korozję. Krzywe polaryzacji dla powłok trójwarstwowych charakteryzują się występowaniem dwóch obszarów pasywacji. Poprawa odporności na korozję jest skutkiem nie tylko tzw. zjawiska blokowania porów w miedzi. Powłoka z Cu działała także jako warstwa protektorowa, modyfikując mechanizm korozji i poprawiając odporność korozyjną powłok.

### 1. Introduction

Electroless nickel (EN) plating is a process for depositing nickel alloy onto a substrate by electrochemical reactions [1]. This process can effectively and economically improve the surface property and corrosion resistance of iron and steel products because of its high wear and corrosion resistance, good lubricity, and excellent thickness uniformity even in recessed areas [2-10]. In contrast to zinc or cadmium coatings that act as sacrificial coatings [11], Ni-P coatings function as a barrier by isolating the substrate from the aggressive environment. The coatings are cathodic to the substrate (steel) because the corrosion potential  $E_{corr}$  is higher than that of the substrate. Galvanic corrosion cells are formed once the pores exist on the coating, thereby severely accelerating the corrosion rate of the anodic substrate. Therefore, Ni-P coatings should be pore-free.

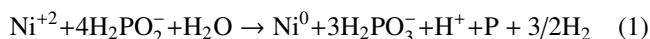
The porosity of Ni-P coatings is affected by surface roughness of the substrate, phosphorus content of the coating, and coating thickness. Ni-P coatings with high phosphorus contents (> 10 wt.%) exhibit lower porosities than those with

low phosphorus contents. Rough substrate surfaces also increase the porosity of the coating, whereas increased coating thicknesses effectively reduce porosity. For relatively smooth substrates with a roughness  $R_a > 5-10 \mu\text{m}$ , the coating thickness ranges from  $12 \mu\text{m}$  to  $15 \mu\text{m}$  to obtain acceptable porosities. A thickness of at least  $25 \mu\text{m}$  is necessary for rough or sandblasted substrates [12, 13]. However, increased coating thicknesses also increases the production cost. Multilayer or interlayer plating effectively modifies the coating properties without increasing the thickness [14-18]. Gu et al. [17] reported that three-layer coatings with electroplated Ni layer inserted between two Ni-P layers exhibited much better corrosion resistance than single-layer coatings. Zeng et al. [18] prepared a double-layer coating that comprised a plasma electrolytic oxidation (PEO) inner layer and a Ni-P outer layer to enhance the corrosion resistance of the magnesium alloy AZ91D. However, few studies have focused on porosity reduction by multilayer plating. The study demonstrates a proposed approach in multilayer plating, which dramatically decreases the porosity and improves the corrosion resistance of coatings.

\* KEY LAB OF LIQUID STRUCTURE AND HEREDITY OF MATERIALS, MINISTRY OF EDUCATION, SHANDONG UNIVERSITY, JINAN 250061, SHANDONG, CHINA

‡ Corresponding author: yzou@sdu.edu.cn

According to Randin and Hintermann [1], the overall reaction of electroless Ni-P plating can be written as follows:



Gas bubbles are produced after the reaction and adsorbed by the substrate, especially at deficient locations. Adsorption of gas bubbles results in isolation of these locations from the plating bath and formation of coating defects [19–21]. In this study, a Cu interlayer was sandwiched by two Ni-P layers to block the holes in the coating. The Cu placed on one side exhibits higher corrosion potential than steel; the Cu on the other side is deposited in the holes of the Ni-P layers by a metal displacement reaction, which easily blocks the holes. The metal displacement of Cu deposition can be represented by Equation (2):



No gas is produced during the process, which prevents the disturbances caused by gas bubbles.  $\text{Cu}^{2+}$  penetrates the pores in the Ni-P inner layer and reacts with metal atoms from the substrate. However, adhesion of the coating deposited by displacement reaction is slightly poor when the Cu layer is directly deposited on the substrate [22, 23]. Thus, the Cu layer was designed for deposition on the Ni-P inner layer rather than on the substrate directly. Given that the Cu layer grew from the pores of the inner layer, it was locked into the inner layer, enhancing its adhesion [18, 24]. The thickness of the Ni-P inner layer is a key parameter for a three-layer coating system. This layer should be thick enough to ensure good adhesion of the Cu layer; the Ni-P inner layer should be thin enough to ensure that  $\text{Cu}^{2+}$  penetrates the layer and contact the substrate. The effect of the thickness of the inner layer was analyzed on the corrosion resistance of the Ni-P/Cu/Ni-P three-layer coating.

## 2. Experimental details

### 2.1. Substrate materials and deposition process

Single-layer and multilayer coatings were prepared on rectangular specimens (15 mm×15 mm×0.8 mm) made of mild steel. The specimens were ground with SiC paper (grade 600) to ensure uniform surface roughness. Substrate pre-treatment was carried out by multi-step process, which included alkaline cleaning, acid pickling, and sensitization. A three-step process was performed to obtain the Ni-P/Cu/Ni-P coating. The specimens were initially immersed in the electroless Ni-P plating bath to obtain the Ni-P inner layer. The Cu interlayer was then deposited by dipping the samples into a Cu plating bath. Finally, the specimens were immersed again in the Ni-P plating bath to yield the outer Ni-P layer. The coating specimens were rinsed with a large volume of deionized water between any two deposition procedures. For Ni-P plating, nickel sulfate and sodium hypophosphite were used as nickel source and reducing agent, respectively [25]. Ni-P plating was performed at a bath temperature of 82°C and pH of 4.5. For Cu deposition,  $\text{CuSO}_4$  was adopted as the main salt in the Cu plating bath. Plating was performed at room temperature, and

the pH of the Ni-P plating bath was adjusted using an aqueous solution of ammonia.

Eleven samples with different thicknesses of Ni-P inner layer were prepared (Table 1). The thickness of the Ni-P layer was controlled by plating time. To observe the surface morphologies and evaluate the properties of the Cu interlayer, Ni-P/Cu double-layer coatings (samples 3 to 5) were prepared and compared with the corresponding single-layer coatings (samples 1 and 2) to identify the characteristics of the Cu interlayer. Samples 7 to 11 were prepared as Ni-P/Cu/Ni-P three-layer coatings. The thickness of the inner layer was increased from sample 7 to sample 11 because the plating time of the inner layer increased from 10 min to 50 min. For comparison, the total deposition time of the Ni-P coating was set at 60 min for three-layer coatings (samples 7 to 11), and sample 6 was plated with a single Ni-P layer coating.

TABLE 1

Coatings prepared in the present experiments

Sample	Coating types	Plating Time (min)
1	Single layer	10 (Ni-P)
2	Single layer	20 (Ni-P)
3	Double-layer	10(Ni-P inner layer)/10(Cu outer layer)
4	Double-layer	20(Ni-P inner layer)/10(Cu outer layer)
5	Double-layer	30(Ni-P inner layer)/10(Cu outer layer)
6	Single layer	60 (Ni-P single layer)
7	Three-layer	10 (Ni-P inner layer)/10 (Cu interlayer)/50 (Ni-P outer layer)
8	Three-layer	20 (Ni-P inner layer)/10 (Cu interlayer)/40 (Ni-P outer layer)
9	Three-layer	30 (Ni-P inner layer)/10 (Cu interlayer)/30 (Ni-P outer layer)
10	Three-layer	40 (Ni-P inner layer)/10 (Cu interlayer)/20 (Ni-P outer layer)
11	Three-layer	50 (Ni-P inner layer)/10 (Cu interlayer)/10 (Ni-P outer layer)

### 2.2. Microstructure analyses and porosity measurements

Surface morphologies of the coatings were analyzed by scanning electron microscope (SEM, Hitachi SU-70, Japan). Chemical composition of the samples was determined by an energy dispersive X-ray spectroscopy (EDS) attached to the SEM. Optical microscopy was performed to investigate the cross-sectional morphology and thickness of the coatings. The crystallographic structure of the coatings was assessed by X-ray diffractometer (XRD) with Cu  $K\alpha$  radiation. Neutral chemical porosity tests were carried out to evaluate the coating porosity of the samples. An aqueous solution of red potassium prussiate was adopted as ferroxy indicator [20, 26]. The corrosive solution attacked the substrate through the pores during the test. Subsequently, the corrosion product passed through the pores, and blue spots appeared on the filter paper because of the reaction with the ferroxy indicator. Given that because the blue spots on the filter paper indicate the coating pores, the porosity of the coating was calculated as the ratio of the total blue spot area to the surface area of the coating. Image

analysis software was used to count the number of pores in the coating and calculate the area of the blue spots.

### 2.3. Electrochemical tests

Electrochemical measurements were carried out in 3.5 wt.% NaCl aqueous solution at room temperature through a classic three-electrode cell, in which the coating sample, Pt plate, and saturated calomel (SCE) functioned as working, counter, and reference electrodes, respectively. The specimen was then sealed with lacquer to leave only one surface (area, 1 cm<sup>2</sup>) exposed to the corrosive medium. The working electrode was cleaned in acetone, agitated ultrasonically, and then rinsed with deionized water. Prior to the polarization curve tests, open circuit potential ( $E_{OCP}$ ) was measured for about 60 min until  $E_{OCP}$  was stabilized. Polarization curves were recorded by scanning the electrode potential from -0.2 V to 1 V with respect to  $E_{OCP}$  at a sweeping rate of 1 mV/s. Corrosion potential ( $E_{corr}$ ) and corrosion current density ( $I_{corr}$ ) were deduced by performing the Tafel extrapolation on the recorded data.

## 3. Results and discussion

### 3.1. Coating characteristics

Surface morphologies of single-layer and double-layer coatings were observed by SEM (Fig. 1). Coating compositions of the samples were determined by EDS and presented in Table 2. The single-layer Ni-P coating plated for 60 min [sample 6, Fig. 1(a)] exhibited a typical nodular structure. The nodules were uniformly and densely distributed, but pores were still present in the coating. Table 2 shows that the Ni-P coating possess a high phosphorous content of 11.34 wt.%. Figs. 1(b) to 1(d) depict the surface morphologies of the double-layer coatings (samples 3 to 5, respectively), and Table 2 tabulates the compositions of the coatings. From samples 3 to 5, the plating time of the Ni-P inner layer increased from 10 min to 30 min (See Table 1). Sample 3 was nearly covered with Cu deposits having a Cu content of 90.77 wt.%. Surface morphology of sample 3 [Fig. 1(b)] was characterized by crystalline particles scattered over the surface, indicating that the deposit was obtained by precipitation of crystalline Cu. Sample 3 exhibited a less smooth surface, and gaps between the particles were bigger compared with those of the Ni-P coating (sample 6). Sample 4 exhibited a reduced Cu content to 43.01 wt.% and a surface covered with spherical nodules and crystalline grains, which respectively represented the Ni-P and Cu deposits. Cu particles evenly distributed on the surface and grew from the pores of the Ni-P inner coating. Sample 5 possessed a Cu content of merely 6.03 wt.%, in which its coating was mostly covered with Ni-P deposits; few Cu particles were observed on the surface of the sample. Furthermore, the Cu particle size of sample 5 was smaller than that of sample 4 because of the reduced pore sizes in the Ni-P inner layer, which was the source of Cu particles. Results revealed that the amount of deposited Cu decreased with increasing thickness of the Ni-P inner layer because the deposition of Cu layer depended on the metal displacement reaction. Pores in the Ni-P inner layer became few, small, and deep by increasing the thickness of

the Ni-P inner layer. Thus, Cu<sup>2+</sup> hardly penetrated the pores and reacted with Fe atoms.

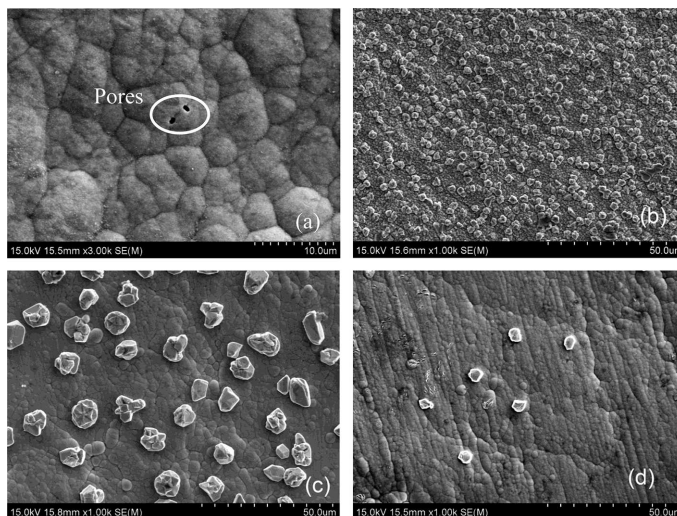


Fig. 1. Surface morphologies of the single layer coating: (a) sample 6 and the double-layer coatings: (b) sample 3, (c) sample 4 and (d) sample 5

TABLE 2  
Chemical composition of the single layer and double-layer coatings determined by EDS analysis

Sample	Ni content (wt.%)	P content (wt.%)	Cu content (wt.%)
3 (double-layer)	8.74	0.49	90.77
4 (double-layer)	51.88	5.10	43.01
5 (double-layer)	83.37	10.60	6.03
6 (single layer)	88.66	11.34	-

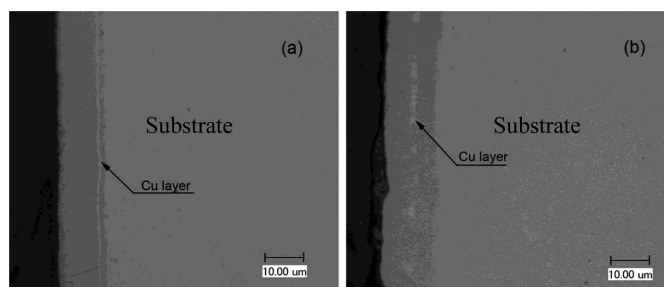


Fig. 2. Cross-sectional morphologies of the three-layer coatings: (a) sample 7 and (b) sample 9 obtained by using optical microscopy

Figure 2 shows the cross-sectional morphologies of the three-layer coatings of samples 7 and 9. The Ni-P inner layer of sample 7 was plated for 10 min, similar to that of sample 3. The three-layer structure comprised Ni-P inner layer, Cu interlayer, and Ni-P outer layer [Fig. 2(a)]. The Cu interlayer was represented as a continuous line with thickness of about 0.6  $\mu\text{m}$ . The thicknesses of the inner layer of sample 7 and the total coating was approximately 2 and 13  $\mu\text{m}$ , respectively. Fig. 2(b) shows the cross-sectional morphologies of sample 9, in which the plating time of the Ni-P inner layer was 30 min. The Cu layer formed a discontinuous line because of the low

porosity that provided less position for Cu deposits. The thickness of the inner layer of sample 9 and the total thickness were about 6.2 and 13  $\mu\text{m}$ , respectively. The reduced amount of deposited Cu with increased thickness of Ni-P inner layer was confirmed from the cross-sectional morphologies. The results implied that the Cu deposit blocked the pores in the inner layer.

### 3.2. Porosity

In this study, porosity was evaluated by neural chemical porosity tests. Figure 3 shows the porosities of the three-layer coatings (samples 7-11). For comparison, the porosity of single-layer coating (sample 6) was also displayed in Fig. 3. Sample 6 had a porosity of 2.28%, whereas the Ni-P/Cu/Ni-P three-layer coatings (samples 7-11) exhibited much lower porosity. The porosities of the three-layer coatings are severely influenced by the plating time of the Ni-P inner layer. Among all the three-layer coatings, sample 7 exhibited the highest porosity (1.03%) because too much Cu was deposited on it given the short deposition time of the Ni-P inner layer. The structure of the crystalline Cu was relatively loose with larger gaps between the grains, which are responsible for the formation of pores. As the plating time of the Ni-P inner layer increased to 20-40 min, the corresponding coatings (samples 8-10) exhibited the lowest porosity, which was below 0.4%. The structure of the interlayer of these coatings was relatively dense compared with that of sample 7 because fewer Cu was deposited in these samples (See Fig. 1). Further, the Cu layer that grew from the pores effectively blocked the pores, thereby significantly decreasing the porosity of the coatings. However, porosity increased as the plating time of the inner layer increased to 40-50 min (samples 10 and 11). The main reason is attributed to the fact that the Cu that can block the pores was hardly deposited because the Ni-P inner layer was too thick. Therefore, the three-layer coatings can decrease the porosity of coatings compared with the single-layer coatings, and the plating time of the Ni-P inner layer should be set to 20-40 min to obtain the lowest porosity.

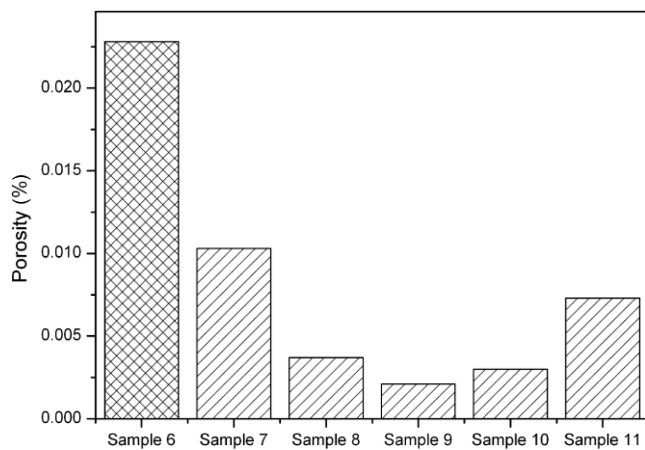


Fig. 3. Porosities of the single layer coating and three-layer coatings

### 3.3. Electrochemical behavior

#### 3.3.1. Potentiodynamic polarization analyses

Fig. 4 shows the polarization curves of the uncoated substrate, single-layer coatings (samples 1 and 2), and double-layer coatings (samples 3 and 4). Electrochemical parameters, such as  $E_{corr}$ ,  $I_{corr}$ , polarization resistance ( $R_p$ ), and anodic Tafel slope ( $\beta_a$ ), were determined from fitting results of the curves (Table 3).

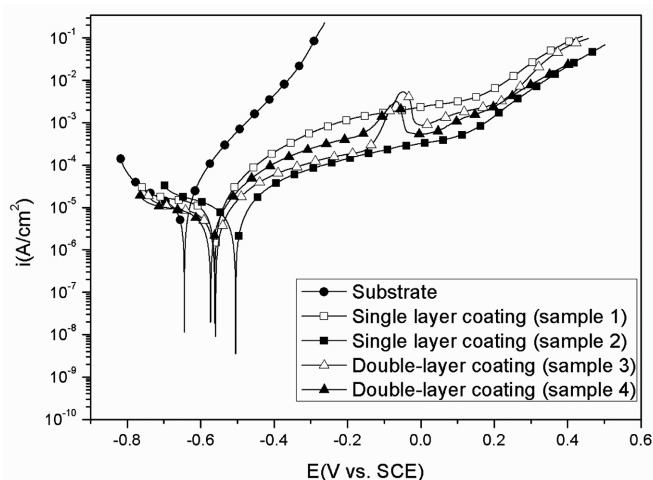


Fig. 4. Potentiodynamic polarization curves of uncoated substrate, single layer coatings and double-layer coatings

TABLE 3

Electrochemical parameters obtained from polarization studies for the uncoated and coated substrates

Sample	$E_{corr}$ (V)	$I_{corr}$ ( $\text{A}/\text{cm}^2$ )	$R_p$ ( $\Omega/\text{cm}^2$ )	$\beta_a$ (mV)
Substrate	-0.644	$4.26 \times 10^{-5}$	1772.6	109.35
1 (Single layer)	-0.562	$2.63 \times 10^{-5}$	2858.9	276.72
2 (Single layer)	-0.505	$1.06 \times 10^{-5}$	4498.6	288.21
3 (Double-layer)	-0.573	$1.34 \times 10^{-5}$	5200.7	262.29
4 (Double-layer)	-0.559	$9.65 \times 10^{-6}$	5384.8	296.09
6 (Single layer)	-0.484	$8.24 \times 10^{-6}$	6419.9	288.29
7 (Three-layer)	-0.488	$4.00 \times 10^{-6}$	8112.3	313.33

The material with low  $E_{corr}$  functioned as the anode of a galvanic corrosion cell, which accelerates the corrosion rate of the material. Thus, the material with high  $E_{corr}$  exhibited high corrosion resistance [27]. Table 3 shows that the uncoated substrate possesses the lowest  $E_{corr}$  (-0.644 V). For single-layer coatings, the  $E_{corr}$  of sample 2 was higher than that of sample 1 because of the increased coating thickness. The double-layer coating (sample 3) exhibited lower  $E_{corr}$  compared with the corresponding single-layer coating (sample 1), which were also observed for samples 2 and 4. However, the plating times of the Ni-P inner layers for samples 1 and 3 were similar. Results revealed that, in contrast to most Cu substrates with higher  $E_{corr}$  than Ni-P coatings [28], the deposited Cu layer by metal displacement reaction possessed lower  $E_{corr}$  than the Ni-P layer. Compared with the Cu substrate, the loose structure of the deposited Cu layer decreased the corrosion potential.

$I_{corr}$  is proportional to the corrosion rate [29]; Table 3 shows that all coated samples exhibited lower  $I_{corr}$  compared with the uncoated substrates, indicating a reduced corrosion rate and increased corrosion resistance. Comparison of  $I_{corr}$  of samples 1 and 2 revealed that  $I_{corr}$  was reduced with increased coating thickness.  $I_{corr}$  of sample 3 was  $1.34 \times 10^{-5}$  A/cm<sup>2</sup>, lower than that of sample 1; but same results were observed for samples 2 and 4. The results suggested that the corrosion rate of the coating was reduced by depositing a Cu outer layer. The plated Cu blocked the micro-pores in the coating, thereby decreasing the possibility for the corrosive medium to attack the substrate through the pores. Therefore, the corrosion rate decreased and the substrate was protected.

The anodic polarization curve of the uncoated substrate showed that the current density rapidly increased as the potential shifted in the anodic direction, indicating that corrosion of the iron substrate was at an active state. For sample 1, the increase in current density slowed down from  $-0.3$  V to  $0.1$  V, implying that corrosion was at a passivation state. The current density rapidly increased above  $0.1$  V, suggesting that the passive film was disintegrated. Passivation plateaus were observed from  $-0.25$  V to  $0.15$  V in the polarization curve of sample 2. The shapes of the polarization curves of the double-layer coatings differed from those of single-layer coatings. For instance, from  $-0.177$  V to  $-0.02$  V, the current density of sample 4 rapidly increased, but sharply decreased thereafter. The result was attributed to the galvanic cell formed between the Cu outer layer and the Ni-P inner layer. As the polarization test proceeded, the Cu outer layer of the Ni-P/Cu double-layer coating gradually eroded, and the Ni-P inner layer was exposed to the electrolyte solution. Thus, corrosion cell was formed; the Cu layer, which exhibited a lower  $E_{corr}$  than Ni-P layer, functioned as the anode. The formation of the corrosion cell rapidly increased the current density. After the Cu layer was completely eroded, Ni-P alloy on the substrate was exposed and the current density decreased. The result indicated that the Cu outer layer first acted as a barrier coating at the corrosion onset, and then performed as a sacrificial coating when the Ni-P alloy was exposed to the electrolyte. Therefore, the Ni-P inner layer and substrate were well protected based on the XRD test of sample 4 after polarization test. Fig. 5 shows that

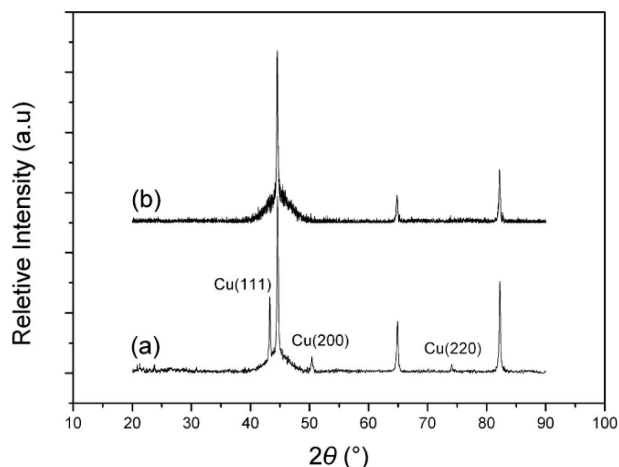


Fig. 5. The XRD patterns of (a) sample 4 before polarization test and (b) sample 4 after polarization test

the amorphous structure of Ni-P was still detected, whereas Cu diffraction peaks were not observed. The non-existence of the diffraction peaks implied that Cu deposits were eliminated prior to Ni-P corrosion.

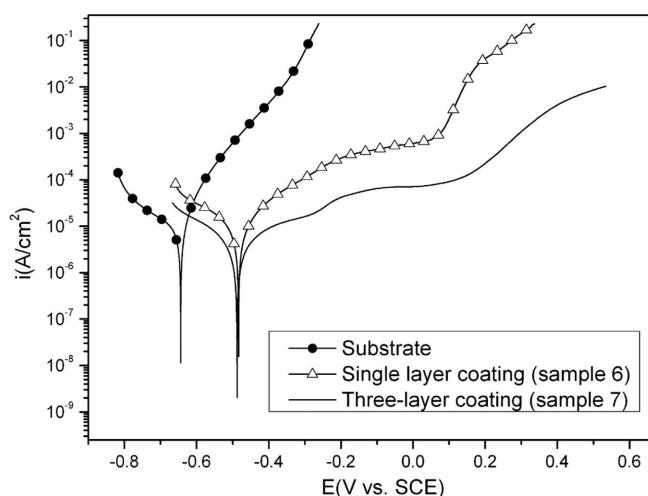


Fig. 6. Potentiodynamic polarization curves of uncoated substrate, single layer coating and three-layer coating

Fig. 6 compares the polarization curves of single-layer coating (sample 6) and three-layer coating (sample 7). Table 3 lists the electrochemical parameters obtained from the curves. The positively shifted  $E_{corr}$  and decreased  $I_{corr}$  of the coated samples implied the improved corrosion resistance in contrast to the uncoated substrate.  $I_{corr}$  of sample 7 was  $4 \times 10^{-6}$  A/cm<sup>2</sup>, which was much lower than that of sample 6. The result indicated that the corrosion rate was reduced by depositing the Cu interlayer between two Ni-P layers because of the significantly decreased porosity of sample 7. A passivation zone was detected from  $-0.02$  V to  $0.06$  V in the polarization curve of sample 6. However, the polarization curve of sample 7 was characterized by two passivation regions from  $-0.4$  V to  $-0.3$  V and from  $-0.15$  V to  $0.1$  V. The first passive film occurred when the Ni-P outer layer corroded from  $-0.4$  V to  $-0.3$  V. The film was then disintegrated, and the Cu interlayer was exposed to the electrolyte. The corrosion cell was formed, and the current density rapidly increased from  $-0.3$  V to  $-0.15$  V. In this region, the Cu interlayer was eliminated as a sacrificial layer based on comparison of the XRD patterns of sample 7 before and after polarization test. Fig. 7 reveals that peaks of crystalline Cu are not detected, and the Ni-P deposit remains after polarization. Thus, the galvanic cell disappeared after elimination of Cu, and the second passive film was formed on the left Ni-P layers from  $-0.15$  V to  $0.1$  V. The corrosion resistance of the Ni-P/Cu/Ni-P three-layer coating was further improved because of the corrosion characteristics of the passivation behavior.

According to the above results, it can be seen that the Cu layer has two roles. One is the plated Cu blocked the micro-pores in the coating, which decrease the porosity of the coating. The second role is to form the galvanic cell with Ni-P layer in corrosion solution, in which Cu interlayer was eliminated as a sacrificial layer to protect the Ni-P matrix. Due to the functions of Cu layer, the corrosion resistances of

the multilayer coatings were greatly improved by introducing a Cu interlayer.

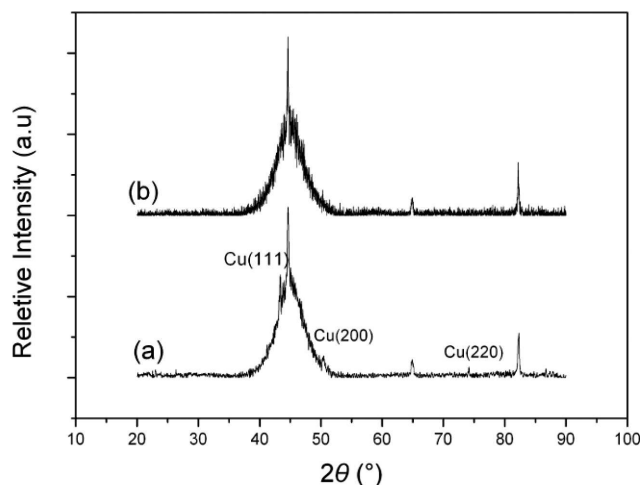


Fig. 7. The XRD patterns of (a) sample 7 before polarization test and (b) sample 7 after polarization test

#### 4. Conclusions

Ni-P/Cu/Ni-P multilayer coatings were prepared and their corrosion resistances were investigated. Crystalline Cu deposits grew from the pores of the amorphous Ni-P inner layer and blocked the pores in the three-layer coating. Experimental results showed that the porosity of three-layer coatings significantly decreased compared with the conventional Ni-P single-layer coating, especially when the plating time of the Ni-P inner layer was set from 20 min to 40 min.  $E_{corr}$  of the Cu layer was lower than that of the Ni-P inner layer. Polarization curves of the multilayer coatings indicated that the Cu layer functioned as a sacrificial coating upon exposure of the corrosion medium with the Ni-P alloy. The results revealed that the corrosion behavior of the Cu interlayer and the dramatically decreased porosity contributed to the improved corrosion resistance of the three-layer coating system.

#### Acknowledgements

This project is supported by National Natural Science Foundation of China (No. 51271099).

#### REFERENCES

[1] G.O. Mallory, J.B. Hajdu, A. Electroplaters, S.F. Society, Electroless plating: fundamentals and applications, The Society, 1990.  
 [2] W. Riedel, Electroless nickel plating, ASM International, 1991.

[3] J.T.W. Jappes, B. Ramamoorthy, P.K. Nair, J. Mater. Process. Technol. **169**, 308 (2005).  
 [4] H. Habazaki, S.Q. Ding, A. Kawashima, K. Asami, K. Hashimoto, A. Inoue, T. Masumoto, Corros. Sci. **29**, 1319 (1989).  
 [5] Q. Zhao, Y. Liu, Corros. Sci. **47**, 2807 (2005).  
 [6] R. Elansezhian, B. Ramamoorthy, P. Kesavan Nair, Surf. Coat. Technol. **203**, 709 (2008).  
 [7] T.S.N.S. Narayanan, I. Baskaran, K. Krishnaveni, S. Parthiban, Surf. Coat. Technol. **200**, 3438 (2006).  
 [8] J.A. Berrios, M.H. Staia, E.C. Hernandez, H. Hintermann, E.S. Puchi, Surface and Coatings Technology **108-109**, 466 (1998).  
 [9] E. Georgiza, J. Novakovic, P. Vassiliou, Surface and Coatings Technology **232**, 432 (2013).  
 [10] P.L. Cavallotti, L. Magagnin, C. Cavallotti, Electrochimica Acta **114**, 805 (2013).  
 [11] W.X. Zhang, Z.H. Jiang, G.Y. Li, Q. Jiang, J.S. Lian, Appl. Surf. Sci. **254**, 4949 (2008).  
 [12] H. Deng, T. I. Met. Finish. **71**, 142 (1993).  
 [13] H. Deng, P. Moller, Plat. Surf. Finish. **81**, 73 (1994).  
 [14] C.-H. Hsu, J.-K. Lu, R.-J. Tsai, Surf. Coat. Technol. **200**, 5725 (2006).  
 [15] C.-H. Hsu, K.-L. Chen, C.-Y. Lee, K.-C. Lu, Surf. Coat. Technol. **204**, 997 (2009).  
 [16] T.S.N.S. Narayanan, K. Krishnaveni, S.K. Seshadri, Mater. Chem. Phys. **82**, 771 (2003).  
 [17] C. Gu, J. Lian, G. Li, L. Niu, Z. Jiang, Surf. Coat. Technol. **197**, 61 (2005).  
 [18] L. Zeng, S. Yang, W. Zhang, Y. Guo, C. Yan, Electrochimica Acta **55**, 3376 (2010).  
 [19] J. Li, Y. Tian, Z. Huang, X. Zhang, Appl. Surf. Sci. **252**, 2839 (2006).  
 [20] F.C. Walsh, C. Ponce de León, C. Kerr, S. Court, B.D. Barker, Surf. Coat. Technol. **202**, 5092 (2008).  
 [21] J. Creus, H. Mazille, H. Idrissi, Surf. Coat. Technol. **130**, 224 (2000).  
 [22] D.C. Ko, S.K. Lee, B.M. Kim, H.H. Jo, H. Jo, J. Mater. Process. Technol. **186**, 22 (2007).  
 [23] W. Song, J. Zhang, Y. Xie, Q. Cong, B. Zhao, J. Colloid Interface Sci. **329**, 208 (2009).  
 [24] Y.I. Chen, J.G. Duh, Surf. Coat. Technol. **48**, 163 (1991).  
 [25] Y.H. Cheng, Y. Zou, L. Cheng, W. Liu, Mater. Sci. Technol. **24**, 457 (2008).  
 [26] P. Ernst, L.P. Wadsworth, G.W. Marshall, T. I. Met. Finish. **75**, 194 (1997).  
 [27] V.K.W. Grips, V. Ezhil Selvi, H.C. Barshilia, K.S. Rajam, Electrochimica Acta **51**, 3461 (2006).  
 [28] G. Liu, L. Yang, L. Wang, S. Wang, L. Chongyang, J. Wang, Surface and Coatings Technology **204**, 3382 (2010).  
 [29] C.-H. Hsu, K.-L. Chen, C.-Y. Lee, K.-C. Lu, Surface and Coatings Technology **204**, 997 (2009).  
 [30] J.N. Balaraju, V. Ezhil Selvi, K.S. Rajam, Materials Chemistry and Physics **120**, 546 (2010).  
 [31] Z. Sharer, J. Sykes, Progress in Organic Coatings **74**, 405 (2012).